

Quantum Computing, Ising formulation, and the Traveling Salesman Problem

Omer Gurevich¹, Maor Matityahu¹, and Tal Mor^{1,2}

¹Computer Science Department, Technion, Haifa, Israel*

²The Helen Diller Quantum Center, Technion, Haifa, Israel

January 1, 2026

Abstract

Ising formulation is important for many NP problems (Lucas, 2014). This formulation enables implementing novel quantum computing methods including Quantum Approximate Optimization Algorithm and Variational Quantum Eigensolver (VQE). Here, we investigate closely the traveling salesman problem (TSP).

First, we present some non-trivial issues related to Ising model view versus a realistic salesman.

Then, focusing on VQE we discuss and clarify the use of: a.– Conventional VQE and how it is relevant as a novel SAT-solver; b.– Qubit efficiency and its importance in the Noisy Intermediate Scale Quantum era; and c.– the relevance and importance of a novel approach named Discrete Quantum Exhaustive Search (Alfassi, Meirom, and Mor, 2024), for enhancing VQE and other methods using mutually unbiased bases.

The approach we present here in details can potentially be extended for analyzing approximating and solving various other NP complete problems. Our approach can also be extended beyond the Ising model and beyond the class NP, for example to the class Quantum Merlin Arthur (QMA) of problems, relevant for quantum chemistry and for general spin problems.

1 Introduction

1.1 Motivation

Quantum computers promise to change the computer science and engineering world. In practice however, there are three major limitations depending on the type of problems: A.– For some problems it is fully believed (and in some case even proven under reasonable assumptions) that quantum computers will

*Email: omergu@campus.technion.ac.il

exponentially outperform classical ones. However, it seems that the tiny needed error-rate, the large number of qubits, and the need for fault-tolerance quantum error correction, limit the applicability in those cases for a decade or maybe even several decades in the future. The most typical and well known examples for that type of problems are factoring large numbers [1] and quantum simulations for various condensed-matter problems [2]. B.– For some problems there is also a great reason to believe that there is an exponential quantum advantage, possibly already in the near future (named NISQ era, noisy intermediate scale quantum era), yet these problems are man-made especially for the purpose of proving the quantum advantage, e.g., see [3–5]. C.– For many other problems [6, 7] there is less theoretical ground (i.e., no proof under any reasonable assumption) for an exponential quantum advantage, yet these problems are of extreme importance, hence we expect a competition between quantum heuristics and classical heuristics in the near future, i.e., in the NISQ era.

Among the approaches relevant for the abovementioned type-C problems, the VQA [8] in general and the VQE in particular, are the leading approaches. VQE is a great method for analyzing problems for which Ising model Hamiltonian or Heisenberg model Hamiltonian can be written.

While it is of course not expected that a quantum computer will solve any NP-complete problem, it is expected to provide the analogue of the many SAT-solvers [9], that we can call LH-solvers, since Local-Hamiltonian is the natural generalization of SAT when extending from NP problems in the classical world to QMA problems in the quantum world [10].

Similarly to the ability of SAT-solvers to solve SAT and many other NP hard and NP complete problems efficiently, either by solving optimal approximations, or by finding and solving easy sub-classes, we expect the same from LH-solvers. Actually, since the quantum space is far beyond the classical one (e.g., for a qubit versus a bit, it is the whole surface of a sphere instead of just two points the north pole and the south pole), we expect to see in the future novel quantum approaches to NP problems, novel quantum-inspired classical approaches to NP problems, and novel quantum approaches to problems that are harder than NP problems, such as finding the ground state energy of chemical molecules (e.g., Density Functional Theory (DFT) method is proven to be QMA complete [11]).

In the classical NP world, exhaustive search on small-size problems is majorly used when planning to find a SAT-solver (or such) for NP problems. Motivated by that approach, discrete quantum exhaustive search (DQES) [12] has been recently suggested (by Alfassi, Meirom, and Mor) and designed for potentially improving quantum algorithms, and potentially solve two big problems of reaching a solution via an iterative optimization process such as VQA: the problems of local minima and of barren plateaus [13, 14].

Our focus here is VQE, for Ising Hamiltonian. And more specifically we focus on the Traveling Salesman Problem (TSP), an extremely important NP-complete problem. Although we focus here on the TSP, the methods we discuss and demonstrated are relevant far beyond the TSP.

1.2 Hamiltonian Path and Hamiltonian Cycle

Given a graph $G = (E, V)$, directed or undirected, a Hamiltonian path is a path that visits every node exactly once. Similarly, Hamiltonian cycle is the same where in addition the path ends at the starting point and returns to the starting node.

Note that in the Hamiltonian cycle, we describe a solution by the order of nodes that define the cycle, and therefore any cyclic permutation is an equivalent solution. Anti-cyclic permutations are also equivalent solutions if the graph is undirected. In Hamiltonian path this symmetry does not appear. In what follows, we use a quantum algorithm to solve problems that are based on the Hamiltonian cycle. By the principles of quantum mechanics, a superposition of such equivalent solutions is also a valid solution, a phenomenon which has no equivalency in the classic world. By fixing a starting point, this degeneracy can be avoided. However, the two-fold degeneracy that appears due to direction in undirected graphs cannot be avoided.

Determining whether a graph G contains a Hamiltonian path (or a cycle) is an NP-complete problem. However, it can be solved in some cases, in many ways. Here, we follow a solution suggested by Lucas [15]. This solution also enables us to construct the path (or cycle) if it exists. Starting with the Hamiltonian path, we denote the vertices by $v = 1, 2, \dots, |V|$, and we denote $|V| := N$. Next, we define binary variables $x_{v,t}$ that take the value 1 if and only if node v is the t^{th} to be visited in the cycle. A proposed solution can be thus represented with an $N \times N$ table that contains the assignments of the variable $x_{v,t}$. For an example of a Hamiltonian path problem instance and a valid solution, see Fig. 1.

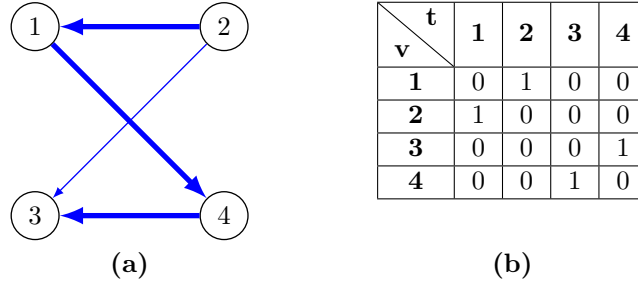


Figure 1: (a) Example of a Hamiltonian path problem instance on a 4-node directed graph. The (unique) solution is in bold. (b) A valid $N \times N$ assignment table representation of the variables $x_{v,t}$

The way to formulate the Hamiltonian cycle problem is very similar to what we did for the Hamiltonian path. To close a cycle, one more node has to be visited. Then we shall use the same binary variables $x_{v,t}$, this time adding N more variables for $x_{v,t=N+1}$. For an example of a Hamiltonian cycle problem instance and a valid solution, according to the proposed naive treatment, see Fig. 2.

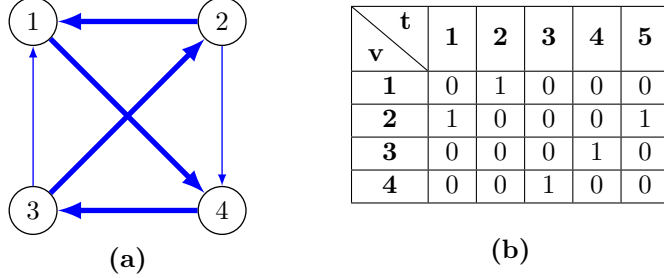


Figure 2: (a) Example of a Hamiltonian cycle problem instance on a 4-node directed graph. A solution (up to cyclic permutation) is in bold. (b) A valid $N \times (N + 1)$ assignment table representation of the variables $x_{v,t}$

As the problem deals with finding a cycle, it is enough to define the cycle with N vertices v_1, \dots, v_N , knowing that $v_{N+1} = v_1$. For a detailed discussion about this way of reducing the number of required variables, as well as other ways, see Secs. 3 and 6.

To solve the Hamiltonian cycle, we begin with formulating the constraints that must hold in a valid solution, using the variables $x_{v,t}$, As was done in [15]:

$$\sum_{t=1}^N x_{v,t} = 1, \quad v = 1, 2, \dots, N, \quad (1)$$

$$\sum_{v=1}^N x_{v,t} = 1, \quad t = 1, 2, \dots, N, \quad (2)$$

$$\sum_{(u,v) \notin E} x_{u,t} x_{v,t+1} = 0, \quad t = 1, 2, \dots, T. \quad (3)$$

From Eq. (1) it is ensured that every node appears exactly once in the path (or cycle), where Eq. (2) states that for any $t = 1, 2, \dots, N$ there must be a single t^{th} node in it. In addition, from Eq. (3) we get that the path (or cycle) is connected. From these expressions (1)-(3) altogether, we see that the Hamiltonian cycle problem is equivalent to finding the values of x_{vt} that minimize the energy of the Hamiltonian:

$$H_A = A \sum_{v=1}^N \left(1 - \sum_{t=1}^N x_{v,t} \right)^2 + A \sum_{t=1}^N \left(1 - \sum_{v=1}^N x_{v,t} \right)^2 + A \sum_{(uv) \notin E} \sum_{t=1}^N x_{u,t} x_{v,t+1}, \quad (4)$$

for some constant $A > 0$, where we identify $N + 1$ with 1, as we mentioned before. This identification allows for using N bits less than without it. For

the Hamiltonian path problem, the last sum should run up to $N - 1$ instead of N . Any assignment of the variables $x_{v,t}$ for which $H_A = 0$ encodes a valid Hamiltonian cycle.

1.3 The traveling salesman problem

In the Travel Salesman Problem (TSP), a salesperson has to visit other cities and return to its city of origin, where every city is visited exactly once, and the distance of the total travel is minimized.

We can model the problem with a weighted graph $G = (E, V)$ (directed or undirected), where every edge $(u, v) \in E$ is assigned a weight (we call it cost) denoted by $c_{uv} \geq 0$. One invalid solution allows, naively, the salesman to fail in his last move, and choose an edge that is cheaper than the one that closes the cycle. Our formulation does not allow this failure, by relying on the Hamiltonian cycle formulation.

Furthermore, in order to slightly decrease the complexity of the problem - we can reduce using some bits (in the table) for the last time step, by employing the cyclic properties of the problem, and specifically, by identifying the initial point with the last point of the cycle while not writing it explicitly in a table. In Fig. 3, we show a TSP instance and its solution, with respect to this efficient formulation

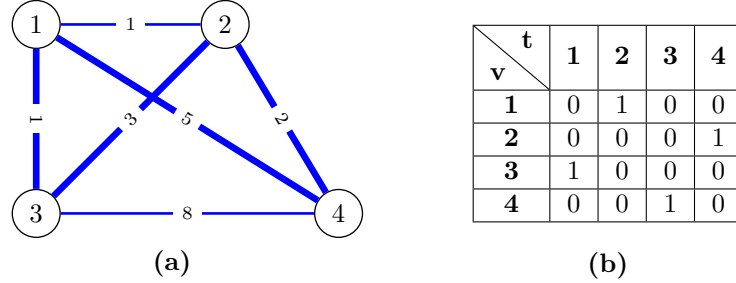


Figure 3: (a) Example of a TSP instance on a 4-node undirected graph. The optimal solution (up to cyclic permutations, as well as two possible directions) is in bold (b) A valid efficient (i.e., $N \times N$) assignment table representation of the variables $x_{v,t}$

As we said, the salesman must traverse a Hamiltonian cycle on the graph, such that the joint cost of the edges in the cycle is minimized. Therefore, we can extend our formulation for the Hamiltonian cycle stated in the previous section, by including this minimization requirement, and obtain an encoding of the problem via a Hamiltonian cost function. To achieve that, we add the term

$$H_B = B \sum_{(uv) \in E} c_{uv} \sum_{t=1}^N x_{u,t} x_{v,t+1}, \quad (5)$$

to the Hamiltonian. The total Hamiltonian that encodes the TSP is therefore given by

$$H_{TSP} = H_A + H_B, \quad (6)$$

with H_A from Eq. (4), where the constants A, B must be chosen such that penalties for bad solutions are high enough, and only valid solutions are energetically preferable. Further details on how these constants are chosen are given for general graphs in Sec. 2, and for the complete graphs in Sec. 2.1.

2 A Note about Penalties in General Graphs

In [15] it was suggested that the condition on A, B from Eq. (6) could be

$$0 < B \max(c_{u,v}) < A. \quad (7)$$

However, we noted that this condition is not sufficient in general. In Fig. 4 we present a counter-example graph, along with its corresponding table assignment of an invalid, yet lowest-cost solution.

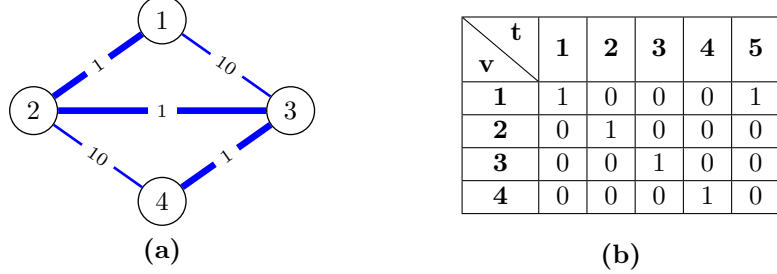


Figure 4: A counter example to correctness of [15] assuming $A = 11, B = 1$. For an efficient formulation, (a) Undirected graph for the TSP instance with optimal solution in bold. By definition, there is also a step from node 5 back to node 1, even though there is no edge joining these two nodes. The only legitimate solutions with node 1 as the starting point are the ones with a cost of 22. (b) A non-efficient yet easy to understand (i.e., $N \times (N + 1)$) assignment table representation for an invalid, yet optimal solution, where a single penalty is paid for the missing edge.

Suppose that $B = 1$ and $A = 11 > B \max(c_{u,v})$. In the counter-example, we have ground-energy $H_{TSP} = 14$, whereas the valid solutions are given by the cycle $1 - 2 - 4 - 3 - 1$ (or the opposite cycle), and they cost $H_{TSP} = 22$.

A safer condition than the one given in Eq. (7) is $0 < N \cdot B \max(c_{u,v}) < A$. For any $A, B > 0$ satisfying this, the optimal solution is guaranteed to be valid.

It may well be that for a complete graph, the condition in [15] is sufficient. An intuitive explanation is given in the next subsection.

We note that the Hamiltonian provided in [15] limits the free will of the salesman. For example, the salesman cannot perform more than N steps, and if performing exactly N steps than his last step must be back to the starting point.

2.1 Penalties in Complete Graphs

In TSP, it is common to assume a complete graph [15]. We now show that under this assumption, for any choice of $A, B > 0$ such that Eq. (7) holds, we are promised that the optimal valid tour indeed minimizes the energy of H_{TSP} . Using the table representation of the assignments leads to an intuitive proof of this fact. The logic is as follows.

In the assignment table, a cell corresponding to some variable $x_{v,t}$ is called *empty* if $x_{v,t} = 0$ and *occupied* otherwise. According to Eqs. (1) and (2), we note that the table of any invalid solution has at least one empty row (or column), or at least one row (or column) with more than one cell occupied. On the other hand, a table with exactly one occupied cell at each row (and therefore also at each column) describes a valid solution. This is due to the fact that all edges exist, so no penalty is caused from Eq. (2) (Alternatively, this constraint could be ignored for a complete graph in the first place).

Assume by contradiction that some invalid solution x' has minimal energy. We can turn it into a valid solution in a way that reduces its energy, arriving at a contradiction. There are many ways to do this. For example, we can go row by row, and when we encounter a row with $k + 1$ full cells, for $k > 0$, We can empty k of these cells, arbitrarily. We may have removed some edges in the process, which lowers the contribution from H_B . Moreover, now a penalty of $k^2 A$ due to the over-occupied row is removed, where new penalties may appear due to columns that are maybe empty. However, these new penalties are no greater than $k^2 A$. So the energy was not increased. Continuing in this fashion for all rows, and then for all columns, we arrive at a table with columns and rows that are either empty or with single-occupation, without increasing the energy. The number of empty rows must be the number of empty columns.

Next, we pick an empty row and fill one of the cells that also belongs to an empty column. We repeat this until exactly each cell is occupied in each row and in each column. At each iteration, two edges e, f are added to the solution, and two violations are corrected. Hence, H_A is reduced by $2A := \Delta H_A$ where H_B is increased by $B(c(e) + c(f)) := \Delta H_B$. By Eq. (7), at each iteration, we only reduced the energy, since $\Delta H_A + \Delta H_B < 0$.

Note that the process ended with a valid tour, and the cost was lowered, where the optimal cycle costs even less. We conclude that the condition in Eq. (7) for the penalty coefficient A is a good choice for complete graphs, where any $B > 0$ works.

2.2 A Note about Realistic Salesman

We note that the Hamiltonian provided in [15] and copied in the introduction here, limits the free will of the salesman. For example, the salesman cannot perform more than N steps, and once performing exactly N steps than his last step must be back to the starting point.

On the other hand, the Hamiltonian formulation allows various things that a realistic salesman cannot do. First, a realistic salesman cannot travel along non-existing path. We suggest to resolve this problem by using a much higher penalty for the third term in the Hamiltonian for the Hamiltonian-cycle. Second, a realistic salesman cannot be in two nodes at the same time. This problem again can be resolved by a much higher penalty relative to the penalty of size A for the realistic salesman returning twice to the same node to save some cost. A last improvement can be to allow a realistic salesman to perform as many steps as he like (more than N , less than N , and add a penalty that grows as the difference from N grows.

Of course any such improvement of the Ising Hamiltonian will add a complexity, so we stick to the Hamiltonian-path based Hamiltonian as Lucas did.

3 A Note about Qubit Efficiency

Saving qubits requires some caution. In Table 1, we show the problem that could result from an efficient representation, by looking at two different solutions, a correct one and a failed one, when described by completing the partial table into an $N \times (N + 1)$ table, for that same undirected graph.

$v \backslash t$	1	2	3	4	5
1	0	1	0	0	0
2	0	0	0	1	0
3	1	0	0	0	1
4	0	0	1	0	0

(a)

$v \backslash t$	1	2	3	4	5
1	0	1	0	0	1
2	0	0	0	1	0
3	1	0	0	0	0
4	0	0	1	0	0

(b)

Table 1: (a) A valid TSP assignment solution described by the full table. (b) An invalid TSP assignment for the same instance, demonstrating violation of constraints via the full table. The demonstration of an efficient yet invalid solution is relevant also for the Hamiltonian cycle problem.

Another invalid situation due to using the efficient representation could be left unnoticed is in case there is no edge connecting node 2 (visited at time step 4) and node 3 (visited at time step 5).

4 Fixing a Starting Point

As mentioned in Sec. 1.2, in Hamiltonian cycle, every Hamiltonian cycle can be expressed in N different ways for directed graphs, and $2N$ ways for undirected graphs. If we add the requirement that the salesman starts from a specific node, say $v = 1$, then this symmetry is broken (there can still be two equivalent cycles for undirected graphs, but this is a $O(1)$ redundancy).

Therefore, we add the constraint $x_{1,1} = 1$, that forces the salesman to start at $v = 1$. The Hamiltonian is updated accordingly:

$$H_{TSP} = A(1 - x_{1,1})^2 + A \sum_{v=1}^N \left(1 - \sum_{t=1}^N x_{v,t} \right)^2 + A \sum_{t=1}^N \left(1 - \sum_{v=1}^N x_{v,t} \right)^2 \\ + A \sum_{(uv) \notin E} \sum_{t=1}^N x_{u,t} x_{v,t+1} + B \sum_{(uv) \in E} c_{uv} \sum_{t=1}^N x_{u,t} x_{v,t+1}, \quad (8)$$

Note that the variable $x_{1,1}$ is now actually a constant by the constraints. This hints that we can encode the problem with less variables, as we will see in Sec. 6. This was also implied from the redundancy in solutions that we mentioned.

5 Ising Form of the Hamiltonian

Before we are able to run a VQA to solve the TSP, we need to rewrite the Hamiltonian from Eq. (8) in Ising form. To achieve this, we express the Hamiltonian as a function of the spin variables $s_{v,t} = \pm 1$ corresponding to eigenvalues of eigenstates $|x_{v,t}\rangle$ of the Pauli-Z operator, rather than as a function of the binary variables.

We obtain this by substituting $x_{u,v} \mapsto \frac{1-s_{u,v}}{2}$ in Eq. (8). Using the fact that for $x^2 = x$ for a binary variable x , we can calculate the different terms in the Hamiltonian with the spin variables. After gathering terms and ignoring the constant part which is irrelevant for optimization, we obtain the Ising Hamiltonian:

$$H_{TSP}^{(\text{Ising})} = A(1 - N) \sum_{v=1}^N \sum_{t=1}^N s_{v,t} \\ + \frac{A}{2} \left(s_{1,1} + \sum_{t=1}^N \sum_{1 \leq u < v \leq N} s_{u,t} s_{v,t} + \sum_{v=1}^N \sum_{1 \leq s < t \leq N} s_{v,s} s_{v,t} \right) \\ + A \sum_{(u,v) \notin E} \sum_{t=1}^N (s_{u,t} s_{v,t+1} - s_{u,t} - s_{v,t+1}) \\ + B \sum_{(u,v) \in E} c_{u,v} \sum_{t=1}^N (s_{u,t} s_{v,t+1} - s_{u,t} - s_{v,t+1}). \quad (9)$$

Note that we could find the constant part, at the cost of complicating the calculation. By having it, the ground state energy is exactly the optimal total

cost. Nevertheless, the groundstate remains the same even if we drop it, and reconstructing the total cost from it is trivial.

6 A Second Note about Qubit Efficiency

We have already discussed how a formulation of the TSP can be wasteful in the number of qubits. In the naive approach, solving the Hamiltonian cycle problem requires $N \times (N + 1)$ qubits, and so does the TSP. However, since we *know* the solution is a cycle, we can identify $N + 1 \equiv 1$, which allows us to omit the spins $s_{v,N+1}$. This identification reduces the number of qubits by N , and leads to the Hamiltonian described in Eq. (6).

Furthermore, we presented another Hamiltonian in Eq. (8) that encodes the same problem but with an additional constraint; the first node in the cycle must be $v = 1$. The set of valid solutions remains the same, since the cycle is unchanged up to rotation. However, fixing the starting point enables an additional reduction in the number of qubits. In the TSP, the starting point is never visited at an intermediate step, so we can eliminate all variables corresponding to such visits. Hence, we are now able to reduce the number of qubits from N^2 to $(N + 1)^2$, since we *know* the values some variables must take (in other words, they are constants):

$$x_{1,t} = \begin{cases} 1 & t = 1 \\ 0 & t \neq 1 \end{cases}, \quad (10)$$

In Table (2) we show which qubits take constant values in the TSP and, therefore, can be ignored, once we fix node 1 as the starting point. This fixation of the starting point is then also demonstrated in the graph, see Fig. 5, where we also present the final (efficient) table.

$v \backslash t$	1	2	3	4	5
1	1	0	0	0	1
2	0	0	1	0	0
3	0	0	0	1	0
4	0	1	0	0	0

Table 2: Table representation of variables in H_{TSP} from Eq. (8). Known variables, with their values specified, are marked in red. The rest of the variables in general are unknown and are marked in green. Here they are taken to match the example in Fig. 3, with the fixed starting point as shown in Fig. 5.

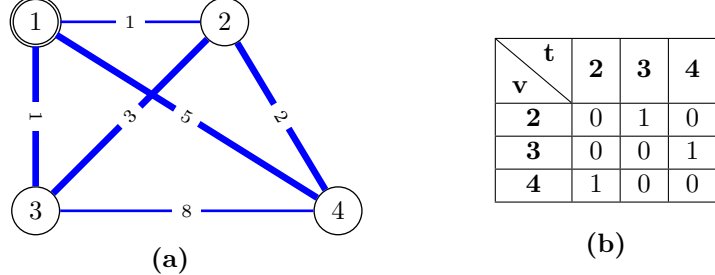


Figure 5: Reduced-qubit representation of after fixing node 1 as the starting point. One solution out of two (namely, up to symmetry of the possible directions from node 1) is in bold.

To obtain a qubit efficient Hamiltonian $H_{TSP}^{\text{efficient}}$ in binary form, we plug Eq. (10) into Eq. (8). Assuming undirected graph ¹, this yields:

$$\begin{aligned}
 H_{TSP}^{\text{efficient}} = & \\
 & A \left[\sum_{v=2}^N \left(1 - \sum_{t=2}^N x_{v,t} \right)^2 + \sum_{t=2}^N \left(1 - \sum_{v=2}^N x_{v,t} \right)^2 \right] \\
 & + A \left[\sum_{(u,v) \notin E} \sum_{t=2}^{N-1} x_{u,t} x_{v,t+1} + \sum_{(1,v) \notin E} \sum_{t=2}^{N-1} (x_{v,2} + x_{u,N}) \right] \\
 & + B \left[\sum_{(u,v) \in E} c_{u,v} \sum_{t=2}^{N-1} x_{u,t} x_{v,t+1} + \sum_{(1,v) \in E} c_{1,v} (x_{v,2} + x_{v,N}) \right]. \tag{11}
 \end{aligned}$$

We also expressed this Hamiltonian in its Ising form, using the same transformation described in Sec. 5. This Ising Hamiltonian is the one used in the numerical experiments of Sec. 7. However, the resulting expression is too lengthy and provides no additional insight, so we omit it.

Overall, we were able to reduce the number of qubits from $N \times (N + 1)$ to $(N - 1)^2$. While this approach does not significantly reduce the space complexity—which remains $O(N^2)$ —the reduction in the number of bits (or qubits, in the context of a quantum algorithm) can still be meaningful for VQAs in the NISQ era. Today’s quantum computers have a limited number of qubits, so even a small reduction in qubit requirements may be critical for enabling algorithms to run on non-trivial instances.

This efficiency in number of variables is also important for classical simulation of quantum algorithms. In the next section, for example, we simulate a TSP instance with 4 cities. Reducing the number of required variables from

¹The expression for directed graph does not differ by much. We show the undirected case for simplicity. Our simulated instances were on undirected graphs.

$4(4 + 1) = 20$ to $(4 - 1)^2 = 9$ significantly reduces the running-time, since it scales exponentially with the number of variables.

7 Numerical Experiments

7.1 DQES Landscape

We now present numerical results for calculating the TSP Hamiltonian energies for unique assignments $\{x_{v,t}\}$. These assignments correspond to the initial states used in the partial-DQES approach, presented in [12]. There it was tested on optimization problems such as the MaxCut and transverse Ising. In partial-DQES, the Ising Hamiltonian energy is calculated for all the following states: For all choices of picking up 3 qubits, we take all mutually unbiased bases (MUBs) elements on these 3-qubits, where the rest of the qubits are at the zero state. There are 9 such bases with 8 basis elements in each. For more details on MUBs, and their importance in quantum information theory, see for example [16–24]. So, for a Hamiltonian on n qubits, we calculate the energy for $\binom{n}{3} \cdot 72$ states.

We now discuss a TSP instance for which we applied the method discussed above, which we refer to as *energy landscape calculation*. In our simulations, we had to find the eigenvalues of the Ising Hamiltonian of interest. We mapped the expressions from Eq. (11), and used their Ising form for the TSP. The mapping was performed in a similar fashion to what we did in Sec. 5 to derive H_{TSP} in its Ising form (Eq. (9)).

We observe that, in general, we should not expect that one of the MUBs states is the eigenstate that corresponds to the optimal solution. However, as our experiments require 3 time-steps only, we expect exactly 3 qubits in the optimal solution to have value of one, where the rest should be zero. As $|111\rangle$ is an MUB state on 3 qubits, we will obtain the optimal solution for one of the states we simulate.

We calculated the DQES landscape for a TSP instance with $N = 4$ nodes, depicted in Fig. 6.

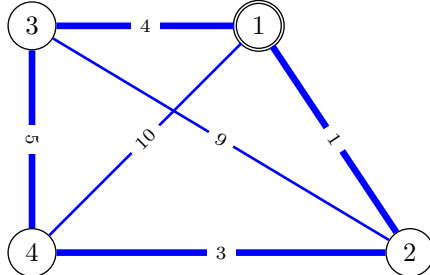


Figure 6: An undirected graph defining a TSP and a instance for our simulations. One solution out of two (namely, up to symmetry of the possible directions from node 1) is in bold. Freedom up to cyclic permutation is removed after fixing node 1 as the starting point.

As was demonstrated in Table (2), the space efficient Hamiltonian which we use, is defined over $(N - 1)^2 = 9$ qubits. We calculate the energy of all initial states of the partial-DQES method on 3 qubits. In Fig. 7 we can see the energy for all such states. Two states yield the minimum energy, which corresponds

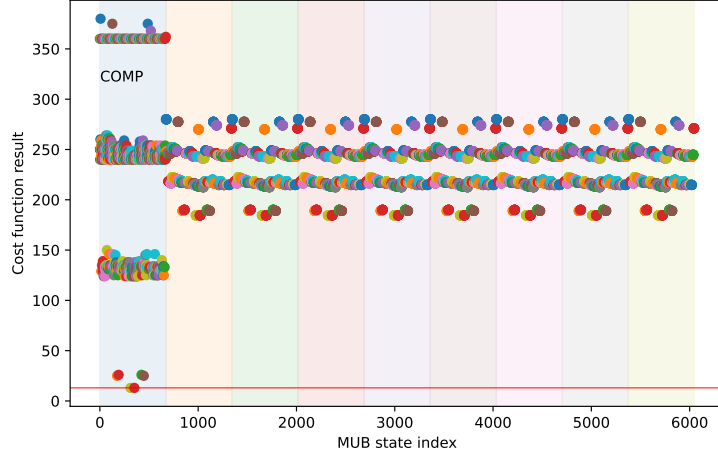


Figure 7: Energy landscape of all partial-DQES initial states on two qubits, for the 4-node TSP instance of Fig. 6. Two degenerate solutions with minimal energy corresponding to the optimal TSP cycles are apparent.

to the optimal TSP solution. These solutions are shown in Table (3), and are given by the cycles $1 - 2 - 4 - 3 - 1$ and $1 - 3 - 4 - 2 - 1$. Denoting the total cost of the travel by C , these two cycles have the same minimal cost $C = 13$. Note that they correspond to the same cycle, but with opposite directions. This degeneracy is expected for undirected graphs, as discussed in Sec. 1.2.

v	t	1	2	3	4	5
1	1	1	0	0	0	1
2	2	0	1	0	0	0
3	3	0	0	0	1	0
4	4	0	0	1	0	0

v	t	1	2	3	4	5
1	1	1	0	0	0	1
2	2	0	0	0	1	0
3	3	0	1	0	0	0
4	4	0	0	1	0	0

Table 3: The two optimal solutions of the TSP instance of Fig. 6.

7.2 VQE Experiment on Top of DQES

The full scheme of DQES, as suggested in [12], involves running the VQE algorithm, starting from all MUB states (up to rotation), or all MUB states on k out of n qubits (with the other qubits potentially taken as $|0\rangle$), in the case of partial-DQES. The idea behind DQES is that MUB states are evenly-spread in the Hilbert space, and therefore initializing VQE from such points can help bypass local minima and barren plateaus, which are the main challenges in VQAs.

Here, we experimented with a computationally faster approach than starting from all the MUB states of the partial-DQES. Instead, we considered starting from a small number k of lowest energy MUB states in the MUB landscape. We are of course not promised that it is always a good thing to do, as maybe a ‘bad’ point is the only one that bypasses a barren plateau. Nevertheless, the intuition behind starting from the best points is straightforward: It is plausible to hope that starting from low energy states which are (in some sense) closer to the ground-state can improve convergence. An additional benefit is that the number of VQE runs is now $k = O(1)$ instead of $O(n)$.

For the TSP defined in Fig. 6, we ran VQE starting from the best $k = 10$ MUB states in the landscape obtained in previous section for the same instance. As a comparison, we also ran VQE with random initializations; an alternative approach used to avoid barren plateaus and local minima (see [25] and [26]), for example). We started from $k = 10$ different random points. The results are shown in Fig. 8.

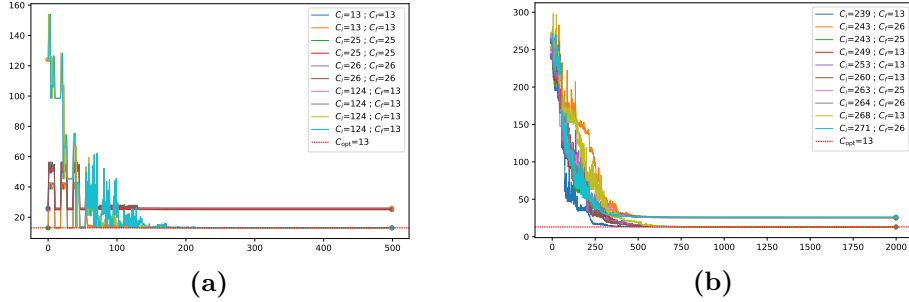


Figure 8: VQE optimization processes starting from (a) the 10 best MUBs (b) 10 random initial points. Initial and final costs are denoted by C_i and C_f respectively. Optimal cost (C_{opt}) appears for comparison.

From Fig. 8 we can tell that 6 out of the 10 VQE runs starting from best MUB states converged, compared to 5 out of the 10 runs starting from random points. More comparisons (and on other problems) are required to deduce a meaningful advantage to either of the methods, but we can see that at least for this TSP instance, both methods are useful in avoiding local minima or barren plateaus.

The results show an additional feature according to Fig. 8. We see that on average, fewer iterations are required for convergence when starting from the best MUB states, compared to starting from random points. This agrees with our intuition, as the best landscape points are closer to the ground-state. This can be another potential advantage of using the method of starting from the best points in the landscape.

Following the standard practice, we also include a VQE run for starting from $|0\rangle^{\otimes n}$. This result shows a successful convergence and is shown in Fig. 9, with the convergence process seen more clearly on a single curve graph. All our VQE results were obtained by running noiseless simulators via Qiskit Python package, using COBYLA as the optimizer and the Efficient-SU(2) circuit (by default), as the ansatz.

8 Discussion and Further Work

In this work we started by clarifying with details the Ising model for the TSP, along with qubit efficiency and we provided various important notes.

We then applied the partial-DQES on small instances of the TSP, a prominent NP-complete problem. We also ran VQE simulations for the same instance. We observed how identifying symmetries in the problem allows for a reduction of the required Hilbert space dimension. Here a constant reduction was achieved. Such a reduction can nevertheless be relevant in the NISQ era, or even in classical simulations, as it allows us to simulate slightly larger instances.

This work is an initial exploration of the DQES method, specifically for the

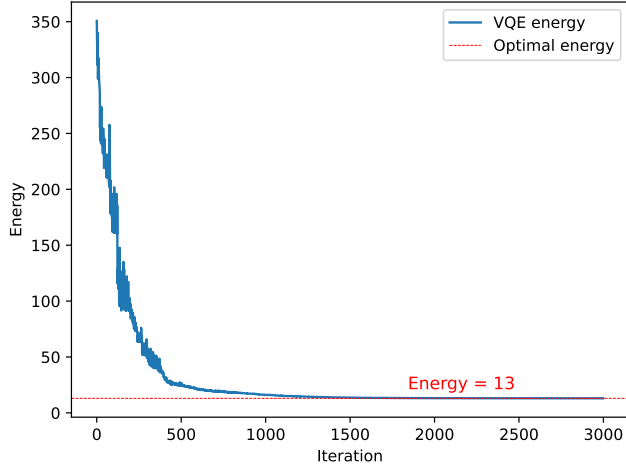


Figure 9: VQE simulation results for the 4-node TSP instance from Fig. 6. Convergence for the known minimal cost (dashed red line) was achieved.

TSP. As such, there are several directions in which we can further investigate:

- **Further comparisons between the DQES method and other methods:** This was already demonstrated here with the standard VQE, but we aim to simulate larger instances of the problem and examine specifically how DQES can help with trainability issues such as barren plateaus and local minima. We can compare with other methods that claim to be effective in avoiding barren plateaus, such as [27]. Comparison to QAOA, or even adapting DQES to QAOA, is a potential direction as well. In addition, we hope to perform experiments with noisy simulators or on real noisy devices.
- **Formulating concrete heuristics for DQES-based SAT- or LH-solvers:** The method we used in our simulations is partial-DQES for $k = 2$ qubits. According to [24], building the quantum circuit that generates MUBs over k qubits can be done efficiently, and even classically, as the gates required are all Clifford gates. The caveat is that the number of MUB states is exponential in k , so the whole procedure of trying all MUB states is not efficient. Despite the inefficiency of naively performing full-DQES on large systems, there are many possibilities worth exploring: (1) There is freedom in how to initialize the other qubits, for example by random initialization in the computational basis, in the whole Hilbert space, or initialization that exploits symmetries or properties of the problem of interest. (2) Knowing how to generate MUB states, we can perform a full DQES on small systems and see if relevant structures (in the energy landscape, for example) can be identified that may help in tackling larger problems. (3) Beyond

initialization, we are interested in developing an optimizer that searches near MUB points, and incorporates problem-specific heuristics as well.

- **Develop and incorporate more qubit efficiency techniques:** By identifying further symmetries or using encoding tricks, such as the logarithmic encoding discussed in Sec. 6 and [15], we may be able to further reduce the number of qubits required for the TSP, or apply such techniques to other problems.
- **Other NP-complete problems:** The Traveling Salesman Problem (TSP) admits many generalizations, such as the Vehicle Routing Problem (VRP), which in turn has numerous variants. These generalizations are especially relevant for real-world applications, for instance in logistics and manufacturing. At the same time, TSP itself, perhaps surprisingly, already plays a role in the context of DNA sequencing [28], a problem of immense importance and one that we wish to study in more detail as well. We believe that considering both generalizations of TSP (such as VRP) and specializations of TSP (such as DNA sequencing) can be beneficial for algorithm design: in the former case, by exposing broader structural principles and symmetries that persist across related problems; in the latter, by exploiting domain-specific structure that may allow for more efficient algorithms.

Ultimately, our exploration of DQES for TSP highlights the potential of symmetry-based and structure-aware approaches in quantum optimization. While many open questions remain, especially regarding scalability and efficiency, the flexibility of the DQES framework—ranging from problem-specific heuristics to generalizations across different NP-complete problems—suggests a rich space for further development. We hope that progress in this direction will help clarify the potential advantages of DQES relative to existing variational methods, and contribute to a deeper understanding of how quantum algorithms can exploit problem structure. We emphasize that DQES for the VRP and for analyzing molecules ground state anaergy is further dealt with by [29, 30].

Acknowledgments

We thank Lev Yohananov for fruitful discussions. T.M and O.G thank the Quantum Computing Consortium of Israel Innovation Authority for financial support. This research project was partially supported by the Helen Diller Quantum Center at the Technion.

References

- [1] P. W. Shor, “Polynomial-time algorithms for prime factorization and discrete logarithms on a quantum computer,” *SIAM review*, vol. 41, no. 2, pp. 303–332, 1999.

- [2] S. Lloyd, “Universal quantum simulators,” *Science*, vol. 273, no. 5278, pp. 1073–1078, 1996.
- [3] S. Aaronson and A. Arkhipov, “The computational complexity of linear optics,” in *Proceedings of the forty-third annual ACM symposium on Theory of computing*, pp. 333–342, 2011.
- [4] F. Arute, K. Arya, R. Babbush, D. Bacon, J. C. Bardin, R. Barends, R. Biswas, S. Boixo, F. G. Brandao, D. A. Buell, *et al.*, “Quantum supremacy using a programmable superconducting processor,” *Nature*, vol. 574, no. 7779, pp. 505–510, 2019.
- [5] E. Pednault, J. A. Gunnels, G. Nannicini, L. Horesh, and R. Wisnieff, “Leveraging secondary storage to simulate deep 53-qubit sycamore circuits,” 2019. arXiv:1910.09534 [quant-ph].
- [6] B. Bauer, S. Bravyi, M. Motta, and G. K.-L. Chan, “Quantum algorithms for quantum chemistry and quantum materials science,” *Chemical reviews*, vol. 120, no. 22, pp. 12685–12717, 2020.
- [7] B. C. Symons, D. Galvin, E. Sahin, V. Alexandrov, and S. Mensa, “A practitioner’s guide to quantum algorithms for optimisation problems,” *Journal of Physics A: Mathematical and Theoretical*, vol. 56, no. 45, p. 453001, 2023.
- [8] M. Cerezo, A. Arrasmith, R. Babbush, S. C. Benjamin, S. Endo, K. Fujii, J. R. McClean, K. Mitarai, X. Yuan, L. Cincio, *et al.*, “Variational quantum algorithms,” *Nature Reviews Physics*, vol. 3, no. 9, pp. 625–644, 2021.
- [9] A. Biere, M. Heule, and H. van Maaren, *Handbook of satisfiability*, vol. 185. IOS press, 2009.
- [10] A. Y. Kitaev, A. Shen, and M. N. Vyalyi, *Classical and quantum computation*. No. 47, American Mathematical Soc., 2002.
- [11] N. Schuch and F. Verstraete, “Computational complexity of interacting electrons and fundamental limitations of density functional theory,” *Nature physics*, vol. 5, no. 10, pp. 732–735, 2009.
- [12] I. Alfassi, D. Meirom, and T. Mor, “Discretized quantum exhaustive search for variational quantum algorithms,” 2024. arXiv:2407.17659 [quant-ph].
- [13] J. R. McClean, S. Boixo, V. N. Smelyanskiy, R. Babbush, and H. Neven, “Barren plateaus in quantum neural network training landscapes,” *Nature communications*, vol. 9, no. 1, p. 4812, 2018.
- [14] M. Larocca, S. Thanasisilp, S. Wang, K. Sharma, J. Biamonte, P. J. Coles, L. Cincio, J. R. McClean, Z. Holmes, and M. Cerezo, “Barren plateaus in variational quantum computing,” *Nature Reviews Physics*, pp. 1–16, 2025.
- [15] A. Lucas, “Ising formulations of many np problems,” *Frontiers in Physics*, vol. 2, 2014.

- [16] N. J. Cerf, M. Bourennane, A. Karlsson, and N. Gisin, “Security of quantum key distribution using d-level systems,” *Physical review letters*, vol. 88, no. 12, p. 127902, 2002.
- [17] T. Durt, “About mutually unbiased bases in even and odd prime power dimensions,” *Journal of Physics A: Mathematical and General*, vol. 38, no. 23, p. 5267, 2005.
- [18] T. Durt, B.-G. Englert, I. Bengtsson, and K. Życzkowski, “On mutually unbiased bases,” *International journal of quantum information*, vol. 8, no. 04, pp. 535–640, 2010.
- [19] D. Bruß, “Optimal eavesdropping in quantum cryptography with six states,” *Physical Review Letters*, vol. 81, no. 14, p. 3018, 1998.
- [20] J. Lawrence, Č. Brukner, and A. Zeilinger, “Mutually unbiased binary observable sets on n qubits,” *Physical Review A*, vol. 65, no. 3, p. 032320, 2002.
- [21] P. Vitória, “Mutually unbiased bases: a brief survey,” 2008.
- [22] P. Butterley and W. Hall, “Numerical evidence for the maximum number of mutually unbiased bases in dimension six,” *Physics Letters A*, vol. 369, no. 1-2, pp. 5–8, 2007.
- [23] Bandyopadhyay, Boykin, Roychowdhury, and Vatan, “A new proof for the existence of mutually unbiased bases,” *Algorithmica*, vol. 34, no. 4, pp. 512–528, 2002.
- [24] W. Yu and W. Dongsheng, “An efficient quantum circuit construction method for mutually unbiased bases in n -qubit systems,” *arXiv preprint arXiv:2311.11698*, 2023.
- [25] J. Kim and Y. Oz, “Quantum energy landscape and circuit optimization,” *Physical Review A*, vol. 106, no. 5, p. 052424, 2022.
- [26] H. Miyahara and V. Roychowdhury, “Ansatz-independent variational quantum classifiers and the price of ansatz,” *Scientific Reports*, vol. 12, no. 1, p. 19520, 2022.
- [27] E. Grant, L. Wossnig, M. Ostaszewski, and M. Benedetti, “An initialization strategy for addressing barren plateaus in parametrized quantum circuits,” *Quantum*, vol. 3, p. 214, 2019.
- [28] A. Sarkar, Z. Al-Ars, and K. Bertels, “Quaser: Quantum accelerated de novo dna sequence reconstruction,” *Plos one*, vol. 16, no. 4, p. e0249850, 2021.
- [29] O. Gurevich, M. Matityahu, T. Mor, and L. Yohananov (in preparation).
- [30] O. Gurevich, T. Mor, and I. Ram (in preparation).